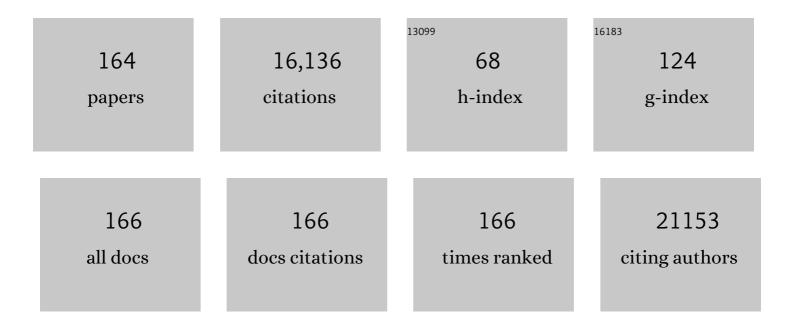
List of Publications by Year in descending order

Source: https://exaly.com/author-pdf/8769659/publications.pdf Version: 2024-02-01



| # | Article | IF | CITATIONS |
|----|--|------|-----------|
| 1 | Persulfate-Induced Three Coordinate Nitrogen (N3C) Vacancies in Defective Carbon Nitride for Enhanced Photocatalytic H2O2 Evolution. Engineering, 2023, 25, 214-221. | 6.7 | 12 |
| 2 | Recent advances in fieldâ€effect transistor sensing strategies for fast and highly efficient analysis of heavy metal ions. Electrochemical Science Advances, 2022, 2, e2100137. | 2.8 | 10 |
| 3 | Highly efficient photocatalytic H2O2 production with cyano and SnO2 co-modified g-C3N4. Chemical Engineering Journal, 2022, 428, 132531. | 12.7 | 86 |
| 4 | H2S sensing under various humidity conditions with Ag nanoparticle functionalized Ti3C2Tx MXene field-effect transistors. Journal of Hazardous Materials, 2022, 424, 127492. | 12.4 | 48 |
| 5 | Selective Removal of Phenolic Compounds by Peroxydisulfate Activation: Inherent Role of Hydrophobicity and Interface ROS. Environmental Science & Technology, 2022, 56, 2665-2676. | 10.0 | 83 |
| 6 | Interconnected Mn-Doped Ni(OH) ₂ Nanosheet Layer for Bifunctional Urea Oxidation and Hydrogen Evolution: The Relation between Current Drop and Urea Concentration during the Long-Term Operation. ACS ES&T Engineering, 2022, 2, 853-862. | 7.6 | 16 |
| 7 | Promotion of Phenol Electro-oxidation by Oxygen Evolution Reaction on an Active Electrode for Efficient Pollution Control and Hydrogen Evolution. Environmental Science & Technology, 2022, 56, 5753-5762. | 10.0 | 22 |
| 8 | Photocatalytic H2O2 production driven by cyclodextrin-pyrimidine polymer in a wide pH range without electron donor or oxygen aeration. Applied Catalysis B: Environmental, 2022, 314, 121485. | 20.2 | 41 |
| 9 | Single-Atom Pt-Functionalized Ti ₃ C ₂ T _{<i>x</i>} Field-Effect Transistor for Volatile Organic Compound Gas Detection. ACS Sensors, 2022, 7, 1874-1882. | 7.8 | 51 |
| 10 | Demand, status, and prospect of antibiotics detection in the environment. Sensors and Actuators B: Chemical, 2022, 369, 132383. | 7.8 | 43 |
| 11 | Enhanced peroxydisulfate oxidation via Cu(III) species with a Cu-MOF-derived Cu nanoparticle and 3D graphene network. Journal of Hazardous Materials, 2021, 403, 123691. | 12.4 | 38 |
| 12 | Thio-groups decorated covalent triazine frameworks for selective mercury removal. Journal of Hazardous Materials, 2021, 403, 123702. | 12.4 | 60 |
| 13 | A review on carbon and non-precious metal based cathode catalysts in microbial fuel cells. International Journal of Hydrogen Energy, 2021, 46, 3056-3089. | 7.1 | 87 |
| 14 | Peroxydisulfate activation by atomically-dispersed Fe-Nx on N-doped carbon: Mechanism of singlet oxygen evolution for nonradical degradation of aqueous contaminants. Chemical Engineering Journal, 2021, 413, 127545. | 12.7 | 102 |
| 15 | Novel insights into the unique intrinsic sensing behaviors of 2D nanomaterials for volatile organic compounds: from graphene to MoS ₂ and black phosphorous. Journal of Materials Chemistry A, 2021, 9, 14411-14421. | 10.3 | 22 |
| 16 | Rapid synthesis of multifunctional β-cyclodextrin nanospheres as alkali-responsive nanocarriers and selective antibiotic adsorbents. Chemical Communications, 2021, 57, 1161-1164. | 4.1 | 11 |
| 17 | Ultrasensitive detection of disinfection byproduct trichloroacetamide in drinking water with Ag nanoprism@MoS2 heterostructure-based electrochemical sensor. Sensors and Actuators B: Chemical, 2021, 332, 129526. | 7.8 | 28 |
| 18 | Label-Free, Fast Response, and Simply Operated Silver Ion Detection with a Ti ₃ C ₂ T <i>_x</i> MXene Field-Effect Transistor. Analytical Chemistry, 2021, 93, 8010-8018. | 6.5 | 35 |

| # | Article | IF | CITATIONS |
|----|--|------|-----------|
| 19 | Bifunctional Electrolyzation for Simultaneous Organic Pollutant Degradation and Hydrogen Generation. ACS ES&T Engineering, 2021, 1, 1360-1368. | 7.6 | 16 |
| 20 | Functionâ€Targeted Lanthanideâ€Anchored Polyoxometalate–Cyclodextrin Assembly: Discriminative Sensing of Inorganic Phosphate and Organophosphate. Advanced Functional Materials, 2021, 31, 2104572. | 14.9 | 25 |
| 21 | Ti3C2Tx MXene sensor for rapid Hg2+ analysis in high salinity environment. Journal of Hazardous Materials, 2021, 418, 126301. | 12.4 | 27 |
| 22 | Rapid and Sensitive Detection of <i>Mycobacterium tuberculosis</i> by an Enhanced Nanobiosensor. ACS Sensors, 2021, 6, 3367-3376. | 7.8 | 26 |
| 23 | The role of Fe-Nx single-atom catalytic sites in peroxymonosulfate activation: Formation of surface-activated complex and non-radical pathways. Chemical Engineering Journal, 2021, 423, 130250. | 12.7 | 88 |
| 24 | Bifunctional Catalytic Cooperativity on Nanoedge: Oriented Ce–Fe Bimetallic Fenton Electrocatalysts for Organic Pollutant Control. ACS ES&T Engineering, 2021, 1, 1618-1632. | 7.6 | 16 |
| 25 | MOF-derived metal-free N-doped porous carbon mediated peroxydisulfate activation via radical and non-radical pathways: Role of graphitic N and C O. Chemical Engineering Journal, 2020, 380, 122584. | 12.7 | 124 |
| 26 | Aeration-assisted sulfite activation with ferrous for enhanced chloramphenicol degradation. Chemosphere, 2020, 238, 124599. | 8.2 | 21 |
| 27 | Nickel-phosphate pompon flowers nanostructured network enables the sensitive detection of microRNA. Talanta, 2020, 209, 120511. | 5.5 | 11 |
| 28 | Tuning layered Fe-doped g-C3N4 structure through pyrolysis for enhanced Fenton and photo-Fenton activities. Carbon, 2020, 159, 461-470. | 10.3 | 111 |
| 29 | Heterogeneous Electro-Fenton catalysis with HKUST-1-derived Cu@C decorated in 3D graphene network. Chemosphere, 2020, 243, 125423. | 8.2 | 47 |
| 30 | One-pot synthesis of ultrafine NiO loaded and Ti3+ in-situ doped TiO2 induced by cyclodextrin for efficient visible-light photodegradation of hydrophobic pollutants. Chemical Engineering Journal, 2020, 402, 126211. | 12.7 | 44 |
| 31 | Highly Enhanced Gas Sensing Performance Using a 1T/2H Heterophase MoS ₂ Field-Effect Transistor at Room Temperature. ACS Applied Materials & Interfaces, 2020, 12, 50610-50618. | 8.0 | 64 |
| 32 | Highly efficient chloramphenicol degradation by UV and UV/H 2 O 2 processes based on LED light source. Water Environment Research, 2020, 92, 2049-2059. | 2.7 | 6 |
| 33 | MnO2 cacti-like nanostructured platform powers the enhanced electrochemical immunobiosensing of cortisol. Sensors and Actuators B: Chemical, 2020, 317, 128134. | 7.8 | 16 |
| 34 | Catalytic Performances of NiCuP@rGO and NiCuN@rGO for Oxygen Reduction and Oxygen Evolution Reactions in Alkaline Electrolyte. ChemistrySelect, 2020, 5, 5855-5863. | 1.5 | 4 |
| 35 | SnO2 nanoparticles incorporated CuO nanopetals on graphene for high-performance room-temperature NO2 sensor. Chemical Physics Letters, 2020, 750, 137485. | 2.6 | 21 |
| 36 | Using a strong chemical oxidant, potassium ferrate (K2FeO4), in waste activated sludge treatment: A review. Environmental Research, 2020, 188, 109764. | 7.5 | 71 |

| # | Article | IF | CITATIONS |
|----|---|------|-----------|
| 37 | Ultrasensitive sensors based on aluminum oxide-protected reduced graphene oxide for phosphate ion detection in real water. Molecular Systems Design and Engineering, 2020, 5, 936-942. | 3.4 | 12 |
| 38 | High Anti-Interference Ti ₃ C ₂ T <i>_x</i> MXene Field-Effect-Transistor-Based Alkali Indicator. ACS Applied Materials & Interfaces, 2020, 12, 32970-32978. | 8.0 | 28 |
| 39 | Exploring the mechanism of the Fe(<scp>iii</scp>)-activated Fenton-like reaction based on a quantitative study. New Journal of Chemistry, 2020, 44, 8952-8959. | 2.8 | 12 |
| 40 | Environmental Analysis with 2D Transition-Metal Dichalcogenide-Based Field-Effect Transistors. Nano-Micro Letters, 2020, 12, 95. | 27.0 | 73 |
| 41 | Field-Effect Transistor Based on Percolation Network of Reduced Graphene Oxide for Real-Time ppb-Level Detection of Lead Ions in Water. ECS Journal of Solid State Science and Technology, 2020, 9, 115012. | 1.8 | 15 |
| 42 | Highly sensitive and selective fluorescent detection of phosphate in water environment by a functionalized coordination polymer. Water Research, 2019, 163, 114883. | 11.3 | 48 |
| 43 | The role of structural elements and its oxidative products on the surface of ferrous sulfide in reducing the electron-withdrawing groups of tetracycline. Chemical Engineering Journal, 2019, 378, 122195. | 12.7 | 24 |
| 44 | Electrochemically Sensing of Trichloroacetic Acid with Iron(II) Phthalocyanine and Zn-Based Metal Organic Framework Nanocomposites. ACS Sensors, 2019, 4, 1934-1941. | 7.8 | 71 |
| 45 | Ultraselective antibiotic sensing with complementary strand DNA assisted aptamer/MoS2 field-effect transistors. Biosensors and Bioelectronics, 2019, 145, 111711. | 10.1 | 68 |
| 46 | Semi-quantitative design of black phosphorous field-effect transistor sensors for heavy metal ion detection in aqueous media. Molecular Systems Design and Engineering, 2019, 4, 491-502. | 3.4 | 17 |
| 47 | Highly luminescent sensing for nitrofurans and tetracyclines in water based on zeolitic imidazolate framework-8 incorporated with dyes. Talanta, 2019, 204, 344-352. | 5.5 | 71 |
| 48 | Hexagonal K ₂ W ₄ O ₁₃ Nanowires for the Adsorption of Methylene Blue. ACS Applied Nano Materials, 2019, 2, 3802-3812. | 5.0 | 14 |
| 49 | Persulfate and zero valent iron combined conditioning as a sustainable technique for enhancing dewaterability of aerobically digested sludge. Chemosphere, 2019, 232, 45-53. | 8.2 | 39 |
| 50 | Nanocomposites of Zr(IV)-Based Metal–Organic Frameworks and Reduced Graphene Oxide for Electrochemically Sensing Ciprofloxacin in Water. ACS Applied Nano Materials, 2019, 2, 2367-2376. | 5.0 | 139 |
| 51 | Prussian blue analog-derived 2D ultrathin CoFe ₂ O ₄ nanosheets as high-activity electrocatalysts for the oxygen evolution reaction in alkaline and neutral media. Journal of Materials Chemistry A, 2019, 7, 7328-7332. | 10.3 | 75 |
| 52 | Recent advances in sensitive and rapid mercury determination with graphene-based sensors. Journal of Materials Chemistry A, 2019, 7, 6616-6630. | 10.3 | 73 |
| 53 | Metal-organic framework-derived core-shell-structured nitrogen-doped CoCx/FeCo@C hybrid supported by reduced graphene oxide sheets as high performance bifunctional electrocatalysts for ORR and OER. Journal of Catalysis, 2019, 371, 185-195. | 6.2 | 78 |
| 54 | Hafnium sulphide-carbon nanotube composite as Pt support and active site-enriched catalyst for high performance methanol and ethanol oxidations in alkaline electrolytes. Journal of Power Sources, 2019, 410-411, 204-212. | 7.8 | 19 |

| # | Article | IF | CITATIONS |
|----|--|------|-----------|
| 55 | Ultratrace antibiotic sensing using aptamer/graphene-based field-effect transistors. Biosensors and Bioelectronics, 2019, 126, 664-671. | 10.1 | 83 |
| 56 | Highly efficient degradation of dimethyl phthalate from Cu(II) and dimethyl phthalate wastewater by EDTA enhanced ozonation: Performance, intermediates and mechanism. Journal of Hazardous Materials, 2019, 366, 378-385. | 12.4 | 33 |
| 57 | Activation of persulfate with metal–organic framework-derived nitrogen-doped porous Co@C nanoboxes for highly efficient p-Chloroaniline removal. Chemical Engineering Journal, 2019, 358, 408-418. | 12.7 | 177 |
| 58 | Rapid detection of nutrients with electronic sensors: a review. Environmental Science: Nano, 2018, 5, 837-862. | 4.3 | 41 |
| 59 | Superior electrocatalysis for hydrogen evolution with crumpled graphene/tungsten disulfide/tungsten trioxide ternary nanohybrids. Nano Energy, 2018, 47, 66-73. | 16.0 | 71 |
| 60 | Strategies for Improving the Performance of Sensors Based on Organic Fieldâ€Effect Transistors. Advanced Materials, 2018, 30, e1705642. | 21.0 | 114 |
| 61 | Decoration of vertical graphene with tin dioxide nanoparticles for highly sensitive room temperature formaldehyde sensing. Sensors and Actuators B: Chemical, 2018, 256, 1011-1020. | 7.8 | 97 |
| 62 | In-situ synthesized TiC@CNT as high-performance catalysts for oxygen reduction reaction. Carbon, 2018, 126, 566-573. | 10.3 | 23 |
| 63 | Real-time electronic sensor based on black phosphorus/Au NPs/DTT hybrid structure: Application in arsenic detection. Sensors and Actuators B: Chemical, 2018, 257, 214-219. | 7.8 | 41 |
| 64 | In Operando Impedance Spectroscopic Analysis on NiO–WO ₃ Nanorod Heterojunction Random Networks for Room-Temperature H ₂ S Detection. ACS Omega, 2018, 3, 18685-18693. | 3.5 | 18 |
| 65 | Enhanced Photocatalytic Removal of Tetrabromobisphenol A by Magnetic CoO@graphene Nanocomposites under Visible-Light Irradiation. ACS Applied Energy Materials, 2018, 1, 2698-2708. | 5.1 | 42 |
| 66 | Real-time and selective detection of nitrates in water using graphene-based field-effect transistor sensors. Environmental Science: Nano, 2018, 5, 1990-1999. | 4.3 | 41 |
| 67 | Graphene Field-Effect Transistor Sensors. , 2018, , 113-132. | | 9 |
| 68 | 3D Edgeâ€Enriched Fe ₃ C@C Nanocrystals with a Core–Shell Structure Grown on Reduced Graphene Oxide Networks for Efficient Oxygen Reduction Reaction. ChemSusChem, 2018, 11, 3292-3298. | 6.8 | 25 |
| 69 | Metal–Organic Framework-Based Sensors for Environmental Contaminant Sensing. Nano-Micro Letters, 2018, 10, 64. | 27.0 | 389 |
| 70 | Organometallic Precursor-Derived SnO ₂ /Sn-Reduced Graphene Oxide Sandwiched Nanocomposite Anode with Superior Lithium Storage Capacity. ACS Applied Materials & Interfaces, 2018, 10, 26170-26177. | 8.0 | 32 |
| 71 | Field-effect transistor biosensors with two-dimensional black phosphorus nanosheets. Biosensors and Bioelectronics, 2017, 89, 505-510. | 10.1 | 206 |
| 72 | Reduced graphene oxide intercalated Co ₂ C or Co ₄ N nanoparticles as an efficient and durable fuel cell catalyst for oxygen reduction. Journal of Materials Chemistry A, 2017, 5. 2972-2980. | 10.3 | 85 |

| # | Article | IF | CITATIONS |
|----|---|-----------|-------------|
| 73 | Ultrasensitive detection of orthophosphate ions with reduced graphene oxide/ferritin field-effect transistor sensors. Environmental Science: Nano, 2017, 4, 856-863. | 4.3 | 28 |
| 74 | Graphene-based electronic biosensors. Journal of Materials Research, 2017, 32, 2954-2965. | 2.6 | 24 |
| 75 | Field-Effect Transistor Biosensor for Rapid Detection of Ebola Antigen. Scientific Reports, 2017, 7, 10974. | 3.3 | 112 |
| 76 | Two-dimensional nanomaterial-based field-effect transistors for chemical and biological sensing. Chemical Society Reviews, 2017, 46, 6872-6904. | 38.1 | 316 |
| 77 | Pulse-Driven Capacitive Lead Ion Detection with Reduced Graphene Oxide Field-Effect Transistor Integrated with an Analyzing Device for Rapid Water Quality Monitoring. ACS Sensors, 2017, 2, 1653-1661. | 7.8 | 57 |
| 78 | Decorating in situ ultrasmall tin particles on crumpled N-doped graphene for lithium-ion batteries with a long life cycle. Journal of Power Sources, 2016, 328, 482-491. | 7.8 | 38 |
| 79 | Nitrogen-boron Dipolar-doped Nanocarbon as a High-efficiency Electrocatalyst for Oxygen Reduction Reaction. Electrochimica Acta, 2016, 222, 481-487. | 5.2 | 37 |
| 80 | Ultrasensitive Mercury Ion Detection Using DNA-Functionalized Molybdenum Disulfide Nanosheet/Gold Nanoparticle Hybrid Field-Effect Transistor Device. ACS Sensors, 2016, 1, 295-302. | 7.8 | 103 |
| 81 | Nanomaterialâ€enabled Rapid Detection of Water Contaminants. Small, 2015, 11, 5336-5359. | 10.0 | 108 |
| 82 | Improving cyclic performance of Si anode for lithium-ion batteries by forming an intermetallic skin. RSC Advances, 2015, 5, 38660-38664. | 3.6 | 22 |
| 83 | Three-dimensional carbon-coated Si/rGO nanostructures anchored by nickel foam with carbon nanotubes for Li-ion battery applications. Nano Energy, 2015, 15, 679-687. | 16.0 | 55 |
| 84 | Metallic CoS ₂ nanowire electrodes for high cycling performance supercapacitors. Nanotechnology, 2015, 26, 494001. | 2.6 | 52 |
| 85 | Amorphous MoS _x Cl _y electrocatalyst supported by vertical graphene for efficient electrochemical and photoelectrochemical hydrogen generation. Energy and Environmental Science, 2015, 8, 862-868. | 30.8 | 183 |
| 86 | Hydrogen Evolution: Perpendicularly Oriented MoSe ₂ /Graphene Nanosheets as Advanced Electrocatalysts for Hydrogen Evolution (Small 4/2015). Small, 2015, 11, 508-508. | 10.0 | 4 |
| 87 | Hybrid Electrocatalysis: An Advanced Nitrogenâ€Doped Graphene/Cobaltâ€Embedded Porous Carbon Polyhedron Hybrid for Efficient Catalysis of Oxygen Reduction and Water Splitting (Adv. Funct. Mater.) Tj ETQq1 | 1 0478431 | 41rgBT /Ove |
| 88 | Emerging energy and environmental applications of vertically-oriented graphenes. Chemical Society Reviews, 2015, 44, 2108-2121. | 38.1 | 269 |
| 89 | Rational design of mesoporous NiFe-alloy-based hybrids for oxygen conversion electrocatalysis. Journal of Materials Chemistry A, 2015, 3, 7986-7993. | 10.3 | 95 |
| 90 | NiO-Microflower Formed by Nanowire-weaving Nanosheets with Interconnected Ni-network Decoration as Supercapacitor Electrode. Scientific Reports, 2015, 5, 11919. | 3.3 | 92 |

| # | Article | IF | CITATIONS |
|-----|--|------|-----------|
| 91 | Real-time detection of mercury ions in water using a reduced graphene oxide/DNA field-effect transistor with assistance of a passivation layer. Sensing and Bio-Sensing Research, 2015, 5, 97-104. | 4.2 | 38 |
| 92 | One-pot synthesis of high-performance Co/graphene electrocatalysts for glucose fuel cells free of enzymes and precious metals. Chemical Communications, 2015, 51, 9354-9357. | 4.1 | 52 |
| 93 | Ultrahigh sensitivity and layer-dependent sensing performance of phosphorene-based gas sensors. Nature Communications, 2015, 6, 8632. | 12.8 | 598 |
| 94 | One-step, continuous synthesis of a spherical Li4Ti5O12/graphene composite as an ultra-long cycle life lithium-ion battery anode. NPG Asia Materials, 2015, 7, e224-e224. | 7.9 | 30 |
| 95 | An Advanced Nitrogenâ€Doped Graphene/Cobaltâ€Embedded Porous Carbon Polyhedron Hybrid for Efficient Catalysis of Oxygen Reduction and Water Splitting. Advanced Functional Materials, 2015, 25, 872-882. | 14.9 | 683 |
| 96 | Three-dimensional graphene-based composites for energy applications. Nanoscale, 2015, 7, 6924-6943. | 5.6 | 241 |
| 97 | A high-performance catalyst support for methanol oxidation with graphene and vanadium carbonitride. Nanoscale, 2015, 7, 1301-1307. | 5.6 | 75 |
| 98 | Perpendicularly Oriented MoSe ₂ /Graphene Nanosheets as Advanced Electrocatalysts for Hydrogen Evolution. Small, 2015, 11, 414-419. | 10.0 | 276 |
| 99 | Nickel oxide hollow microsphere for non-enzyme glucose detection. Biosensors and Bioelectronics, 2014, 54, 251-257. | 10.1 | 208 |
| 100 | Metalâ^'Organic Frameworkâ€Derived Nitrogenâ€Doped Coreâ€Shellâ€Structured Porous Fe/Fe ₃ C@C Nanoboxes Supported on Graphene Sheets for Efficient Oxygen Reduction Reactions. Advanced Energy Materials, 2014, 4, 1400337. | 19.5 | 512 |
| 101 | Nanocarbon-based gas sensors: progress and challenges. Journal of Materials Chemistry A, 2014, 2, 5573. | 10.3 | 202 |
| 102 | Controllable Synthesis of Hollow Si Anode for Long ycleâ€Life Lithiumâ€Ion Batteries. Advanced Materials, 2014, 26, 4326-4332. | 21.0 | 193 |
| 103 | Hierarchical Nanohybrids with Porous CNT-Networks Decorated Crumpled Graphene Balls for Supercapacitors. ACS Applied Materials & amp; Interfaces, 2014, 6, 9881-9889. | 8.0 | 94 |
| 104 | High-performance bi-functional electrocatalysts of 3D crumpled graphene–cobalt oxide nanohybrids for oxygen reduction and evolution reactions. Energy and Environmental Science, 2014, 7, 609-616. | 30.8 | 605 |
| 105 | Enzymeless Glucose Detection Based on CoO/Graphene Microsphere Hybrids. Electroanalysis, 2014, 26, 1326-1334. | 2.9 | 48 |
| 106 | Instantaneous Reduction of Graphene Oxide Paper for Supercapacitor Electrodes with Unimpeded Liquid Permeation. Journal of Physical Chemistry C, 2014, 118, 13493-13502. | 3.1 | 19 |
| 107 | Hydrothermal synthesis of vanadium nitride and modulation of its catalytic performance for oxygen reduction reaction. Nanoscale, 2014, 6, 9608. | 5.6 | 93 |
| 108 | Synthesizing Nitrogen-Doped Activated Carbon and Probing its Active Sites for Oxygen Reduction Reaction in Microbial Fuel Cells. ACS Applied Materials & 2014, 10, 7464-7470. | 8.0 | 157 |

| # | Article | IF | CITATIONS |
|-----|---|------|-----------|
| 109 | Green preparation of reduced graphene oxide for sensing and energy storage applications. Scientific Reports, 2014, 4, 4684. | 3.3 | 433 |
| 110 | Graphene Coupled with Nanocrystals: Opportunities and Challenges for Energy and Sensing Applications. Journal of Physical Chemistry Letters, 2013, 4, 2441-2454. | 4.6 | 80 |
| 111 | Effects of N and F doping on structure and photocatalytic properties of anatase TiO2 nanoparticles. RSC Advances, 2013, 3, 16657. | 3.6 | 43 |
| 112 | TiO2 nanoparticles-decorated carbon nanotubes for significantly improved bioelectricity generation in microbial fuel cells. Journal of Power Sources, 2013, 234, 100-106. | 7.8 | 136 |
| 113 | CNT@TiO2 nanohybrids for high-performance anode of lithium-ion batteries. Nanoscale Research Letters, 2013, 8, 499. | 5.7 | 25 |
| 114 | Nitrogen-doped graphene–vanadium carbide hybrids as a high-performance oxygen reduction reaction electrocatalyst support in alkaline media. Journal of Materials Chemistry A, 2013, 1, 13404. | 10.3 | 50 |
| 115 | Hierarchical vertically oriented graphene as a catalytic counter electrode in dye-sensitized solar cells. Journal of Materials Chemistry A, 2013, 1, 188-193. | 10.3 | 85 |
| 116 | Influence of partial substitution of Mo for Cr on structure and hydrogen storage characteristics of non-stoichiometric Laves phase TiCrB0.9 alloy. International Journal of Hydrogen Energy, 2013, 38, 11955-11963. | 7.1 | 10 |
| 117 | Single-walled carbon nanotube field-effect transistors with graphene oxide passivation for fast, sensitive, and selective proteindetection. Biosensors and Bioelectronics, 2013, 42, 186-192. | 10.1 | 40 |
| 118 | Silicon nanotube anode for lithium-ion batteries. Electrochemistry Communications, 2013, 29, 67-70. | 4.7 | 236 |
| 119 | Indium-doped SnO2 nanoparticle–graphene nanohybrids: simple one-pot synthesis and their selective detection of NO2. Journal of Materials Chemistry A, 2013, 1, 4462. | 10.3 | 129 |
| 120 | Controllable synthesis of silver nanoparticle-decorated reduced graphene oxide hybrids for ammonia detection. Analyst, The, 2013, 138, 2877. | 3.5 | 125 |
| 121 | Ultrasonic-assisted self-assembly of monolayer graphene oxide for rapid detection of Escherichia coli bacteria. Nanoscale, 2013, 5, 3620. | 5.6 | 82 |
| 122 | Direct Growth of Vertically-oriented Graphene for Field-Effect Transistor Biosensor. Scientific Reports, 2013, 3, 1696. | 3.3 | 173 |
| 123 | Crumpled Nitrogenâ€Đoped Graphene Nanosheets with Ultrahigh Pore Volume for Highâ€Performance Supercapacitor. Advanced Materials, 2012, 24, 5610-5616. | 21.0 | 880 |
| 124 | Ultrafast hydrogen sensing through hybrids of semiconducting single-walled carbon nanotubes and tin oxide nanocrystals. Nanoscale, 2012, 4, 1275. | 5.6 | 51 |
| 125 | Tuning gas-sensing properties of reduced graphene oxide using tin oxide nanocrystals. Journal of Materials Chemistry, 2012, 22, 11009. | 6.7 | 274 |
| 126 | Ag nanocrystal as a promoter for carbon nanotube-based room-temperature gas sensors. Nanoscale, 2012, 4, 5887. | 5.6 | 71 |

| # | Article | IF | CITATIONS |
|-----|--|------|-----------|
| 127 | Hg(II) Ion Detection Using Thermally Reduced Graphene Oxide Decorated with Functionalized Gold Nanoparticles. Analytical Chemistry, 2012, 84, 4057-4062. | 6.5 | 224 |
| 128 | Modulating Gas Sensing Properties of CuO Nanowires through Creation of Discrete Nanosized p–n Junctions on Their Surfaces. ACS Applied Materials & Interfaces, 2012, 4, 4192-4199. | 8.0 | 125 |
| 129 | A General Approach to One-Pot Fabrication of Crumpled Graphene-Based Nanohybrids for Energy Applications. ACS Nano, 2012, 6, 7505-7513. | 14.6 | 201 |
| 130 | Binding Sn-based nanoparticles on graphene as the anode of rechargeable lithium-ion batteries. Journal of Materials Chemistry, 2012, 22, 3300. | 6.7 | 97 |
| 131 | Controllable photoelectron transfer in CdSe nanocrystal–carbon nanotube hybrid structures. Nanoscale, 2012, 4, 742-746. | 5.6 | 15 |
| 132 | Graphene oxide and its reduction: modeling and experimental progress. RSC Advances, 2012, 2, 2643. | 3.6 | 463 |
| 133 | Nitrogenâ€Enriched Coreâ€Shell Structured Fe/Fe ₃ Câ€C Nanorods as Advanced Electrocatalysts for Oxygen Reduction Reaction. Advanced Materials, 2012, 24, 1399-1404. | 21.0 | 517 |
| 134 | Nitrogen-Enriched Core-Shell Structured Fe/Fe3C-C Nanorods as Advanced Electrocatalysts for Oxygen Reduction Reaction (Adv. Mater. 11/2012). Advanced Materials, 2012, 24, 1398-1398. | 21.0 | 8 |
| 135 | Vertically oriented graphene sheets grown on metallic wires for greener corona discharges: lower power consumption and minimized ozone emission. Energy and Environmental Science, 2011, 4, 2525. | 30.8 | 66 |
| 136 | Selective Deposition of CdSe Nanoparticles on Reduced Graphene Oxide to Understand Photoinduced Charge Transfer in Hybrid Nanostructures. ACS Applied Materials & Interfaces, 2011, 3, 2703-2709. | 8.0 | 25 |
| 137 | Carbon Nanotube with Chemically Bonded Graphene Leaves for Electronic and Optoelectronic Applications. Journal of Physical Chemistry Letters, 2011, 2, 1556-1562. | 4.6 | 190 |
| 138 | A new reducing agent to prepare single-layer, high-quality reduced graphene oxide for device applications. Nanoscale, 2011, 3, 2849. | 5.6 | 99 |
| 139 | Highly sensitive protein sensor based on thermally-reduced graphene oxide field-effect transistor. Nano Research, 2011, 4, 921-930. | 10.4 | 84 |
| 140 | Growth of carbon nanowalls at atmospheric pressure for one-step gas sensor fabrication. Nanoscale Research Letters, 2011, 6, 202. | 5.7 | 123 |
| 141 | Metal Nitride/Graphene Nanohybrids: General Synthesis and Multifunctional Titanium Nitride/Graphene Electrocatalyst. Advanced Materials, 2011, 23, 5445-5450. | 21.0 | 171 |
| 142 | Understanding growth of carbon nanowalls at atmospheric pressure using normal glow discharge plasma-enhanced chemical vapor deposition. Carbon, 2011, 49, 1849-1858. | 10.3 | 120 |
| 143 | Note: Continuous synthesis of uniform vertical graphene on cylindrical surfaces. Review of Scientific Instruments, 2011, 82, 086116. | 1.3 | 8 |
| 144 | Specific Protein Detection Using Thermally Reduced Graphene Oxide Sheet Decorated with Gold Nanoparticleâ€Antibody Conjugates. Advanced Materials, 2010, 22, 3521-3526. | 21.0 | 444 |

| # | Article | IF | CITATIONS |
|-----|--|------|-----------|
| 145 | Specific biosensing using carbon nanotubes functionalized with gold nanoparticle–antibody conjugates. Carbon, 2010, 48, 479-486. | 10.3 | 39 |
| 146 | One-dimensional tungsten oxide growth through a grain-by-grain buildup process. Chemical Physics Letters, 2010, 485, 64-68. | 2.6 | 11 |
| 147 | The effect of Ag nanoparticle loading on the photocatalytic activity of TiO2 nanorod arrays. Chemical Physics Letters, 2010, 485, 171-175. | 2.6 | 68 |
| 148 | Protein Viability on Au Nanoparticles during an Electrospray and Electrostatic-Force-Directed Assembly Process. Journal of Nanomaterials, 2010, 2010, 1-6. | 2.7 | 1 |
| 149 | Nanoscale Discharge Electrode for Minimizing Ozone Emission from Indoor Corona Devices. Environmental Science & Technology, 2010, 44, 6337-6342. | 10.0 | 32 |
| 150 | Facile, noncovalent decoration of graphene oxide sheets with nanocrystals. Nano Research, 2009, 2, 192-200. | 10.4 | 145 |
| 151 | Carbon-nanotube-assisted transmission electron microscopy characterization of aerosol nanoparticles. Journal of Aerosol Science, 2009, 40, 180-184. | 3.8 | 5 |
| 152 | Microstructural analysis of Ga2S3–2MCl (M = K, Rb, Cs) glasses using Raman scattering. Journal of Non-Crystalline Solids, 2008, 354, 1175-1178. | 3.1 | 1 |
| 153 | New chalcohalide glasses from the GeS2–In2S3–CsCl system. Journal of Non-Crystalline Solids, 2008, 354, 1303-1307. | 3.1 | 11 |
| 154 | Microstructure and thermal properties of the GeS2–In2S3–CsI glassy system. Journal of Non-Crystalline Solids, 2008, 354, 1298-1302. | 3.1 | 12 |
| 155 | Coating carbon nanotubes with colloidal nanocrystals by combining an electrospray technique with directed assembly using an electrostatic field. Nanotechnology, 2008, 19, 455610. | 2.6 | 18 |
| 156 | Fabrication and characterization of microwave immunosensors based on organic semiconductors with nanogold-labeled antibody. , 2008, 2008, 2381-4. | | 2 |
| 157 | RIPENING OF SILVER NANOPARTICLES ON CARBON NANOTUBES. Nano, 2007, 02, 149-156. | 1.0 | 26 |
| 158 | Structure dependence of ultrafast third-order optical nonlinearity for GeS2–In2S3–CsI chalcohalide glasses. Solid State Communications, 2007, 142, 453-456. | 1.9 | 17 |
| 159 | Mechanism of electron beam poled SHG in 0.95GeS2·0.05In2S3 chalcogenide glasses. Journal of Physics and Chemistry of Solids, 2007, 68, 158-161. | 4.0 | 16 |
| 160 | Raman spectroscopic analysis of GeS2–Ga2S3–PbI2 chalcohalide glasses. Spectrochimica Acta - Part A: Molecular and Biomolecular Spectroscopy, 2007, 67, 1351-1356. | 3.9 | 28 |
| 161 | Micro-structural study of the GeS2–In2S3–KCl glassy system by Raman scattering. Spectrochimica Acta - Part A: Molecular and Biomolecular Spectroscopy, 2006, 64, 1039-1045. | 3.9 | 12 |
| 162 | Raman scattering studies of the Ge–In sulfide glasses. Solid State Communications, 2006, 137, 408-412. | 1.9 | 49 |

| # | Article | IF | CITATIONS |
|-----|--|-----|-----------|
| 163 | Formation and properties of the GeS2–In2S3–KCl new chalcohalide glassy system. Materials Letters, 2006, 60, 741-745. | 2.6 | 20 |
| 164 | Raman scattering studies of the GeS2–Ga2S3–CsCl glassy system. Solid State Communications, 2005, 133, 327-332. | 1.9 | 53 |